Supplementary material to accompany the article "Universal condensation threshold dependence on pump beam size for exciton-polaritons"

Oleg I. Utesov, Min Park, Daegwang Choi, Soohong Choi, Suk In Park, Sooseok Kang, Jin Dong Song, Alexey N. Osipov, Alexey V. Yulin, Yong-Hoon Cho, Hyoungsoon Choi, Igor S. Aronson, and Sergei V. Koniakhin

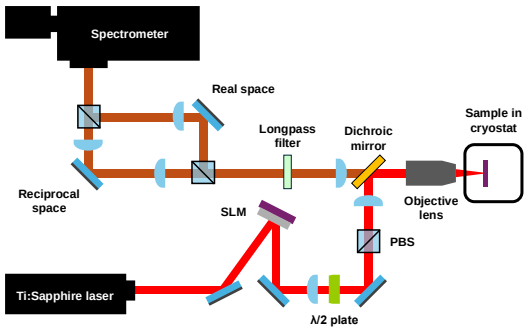

FIG. S1. Scheme of the experimental setup used in the present study.

EXPERIMENTAL

Our experimental setup is schematically illustrated in Fig. S1. Some details of low excitation energy photoluminescence measurements for relatively large laser spot sizes are presented in Fig. S2. Using laser powers well below the condensation threshold allows determining the microcavity Q-factor as a ratio of the peak position to the full width at half maximum.

Energy-resolved emission spectra for various pumping powers and relatively small spot size are shown in Fig. S3 for the KAIST 1 sample. Under weak pumping, the spectrum corresponds to the bare polariton modes. An increase in the pumping leads to the condensate formation. The emission energy narrows at a certain value corresponding to the blueshift due to interaction with other quasi-particles and the size-quantization effect. At yet stronger pumps the strong coupling of excitons and photons is presumably lost and the system acts as a usual photonic laser.

Frequencies corresponding to the maxima of emission spectra for all three samples and various pumping powers as well as corresponding spectral line widths are presented in Figs. S4, S5, and S6. In all the samples we observe a gradual change in these properties upon varying the pump spot size which indicates tunability of exciton-polariton condensates therein. Noteworthy, the KIST sample demonstrates a significant decrease in the spectral line broadening upon condensation (a similar effect was first reported in Ref. [1]).

THEORY

Below we present our theoretical approach with all necessary details.

Effective complex Ginzburg-Landau equation

Our theory is designed to discuss incoherent pumping experiments. We start with the conventional semi-phenomenological approach based on the system of equations [2, 3]

$$\partial_t n_R = P(\mathbf{r},t) - \gamma_R n_R - R(n_R)|\psi|^2, \tag{S1}$$

$$i\hbar\partial_t\psi = \left[-\frac{\hbar^2}{2m}(1-i\beta)\nabla^2 + g_C|\psi|^2 + g_R n_R + \frac{i\hbar}{2}[R(n_R)-\gamma_C]\right]\psi. \tag{S2}$$

Here n_R is the density of particles in the reservoir, $P(\mathbf{r},t)$ is the pumping profile related to the laser intensity spatial distribution, γ_R is the reservoir damping parameter, $R(n_R)$ describes the efficiency of polariton relaxation from the reservoir to the condensate described by the wave function ψ. Below, we will assume the linear dependence $R(n_R) = R_{\text{SC}} n_R$. Next, m is the polariton effective mass, β is related to the momentum dependence of the polariton lifetime (see Ref. [4]), g_C and g_R describe the intra-condensate and condensate-reservoir repulsion, respectively, and γ_C is the condensate polariton damping rate. Henceforth, we will assume $\beta > 0$ since the opposite case leads to a short-wavelength instability which can be "cured" by considering polariton dispersion non-parabolicity.

The basic understanding of the physics described by Eqs. (S1) and (S2) comes from consideration of the homogeneous pumping density $P(\mathbf{r},t) = P_{\text{TH}}$ at the threshold. In that case $\psi = 0$, the reservoir density is constant $n_R^{(0)} = P_{\text{TH}}/\gamma_R$ and the threshold pumping density is determined by the system parameters as $P_{\text{TH}} = \gamma_C\gamma_R/R_{\text{SC}}$. In order to observe the condensation, one should use $P > P_{\text{TH}}$. Furthermore, if the pumping function $P(\mathbf{r},t)$ is inhomogeneous (for instance, Gaussian) the threshold power density is different (larger) than the one of the homogeneous case. This issue is addressed in detail in the present study.

For the analytical treatment, we measure all densities in the units of $n_R^{(0)}$ introduced above which is characteristic of

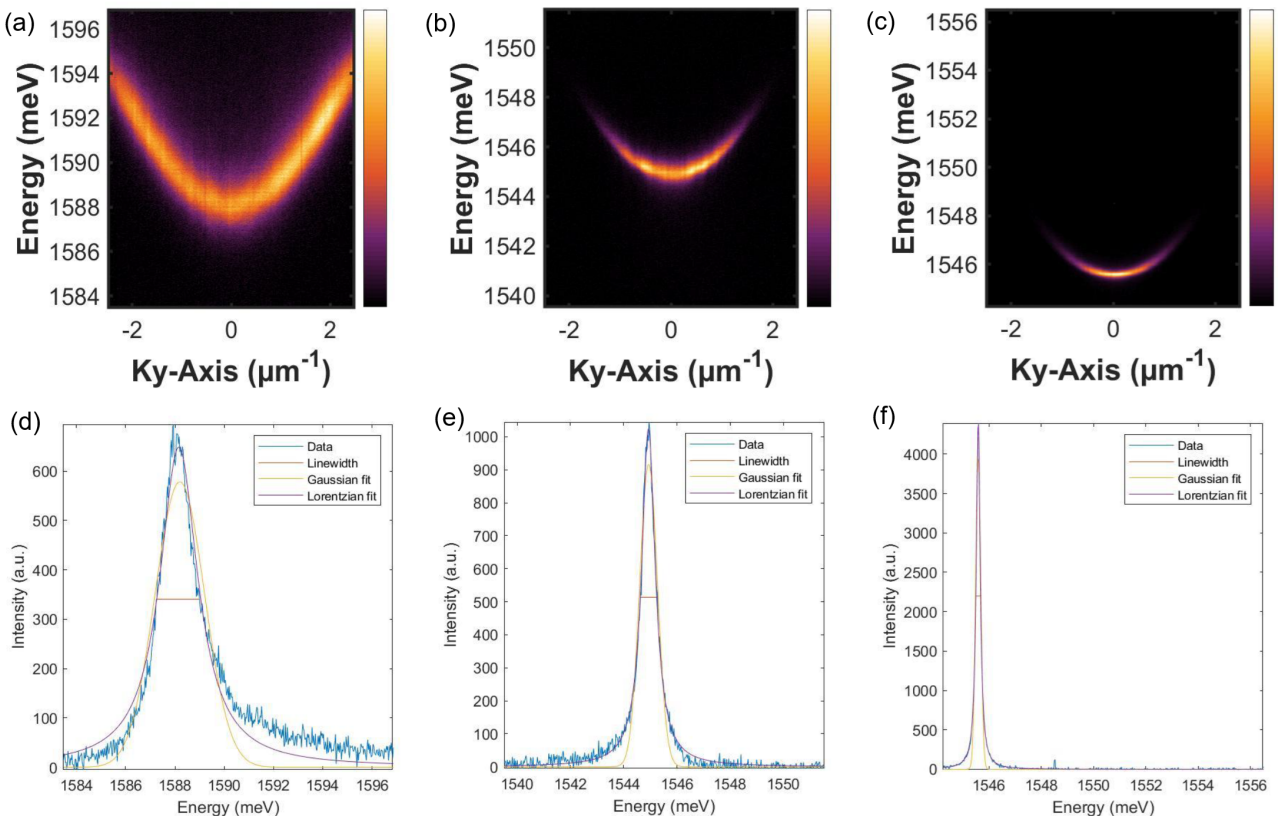

FIG. S2. Energy resolved low pumping power photoluminescence measurements. Fit of the zero-momentum cut with the Lorentzian curve yields the maximum position ω_0 and the broadening γ_L. One of the crucial parameters for the condensation – microcavity Q-factor – is conventionally defined as ω_0/γ_L.

the given sample. Then, the condensate wave function becomes $A = \psi/\sqrt{n_R^{(0)}}$. It is also convenient to measure distances in the units of $\xi = \hbar/\sqrt{2mg_C n_R^{(0)}}$ and times in units of $\tau = \hbar/g_C n_R^{(0)}$. After some calculations we rewrite Eqs. (S1) and (S2) as follows

$$\partial_t n_R = \frac{\gamma_R}{\gamma_C}\varkappa\left[P(\mathbf{r},t) - n_R\right] - \varkappa n_R|A|^2, \tag{S3}$$

$$i\partial_t A = \left[-(1-i\beta)\nabla^2 + |A|^2 + \frac{g_R}{g_C}n_R + \frac{i\varkappa}{2}(n_R - 1)\right]A. \tag{S4}$$

where time and space variables are now dimensionless as well as n_R, A, and $P(\mathbf{r},t)$; the latter is measured in the units of P_{TH}. We also introduced the parameter

$$\varkappa = \frac{\hbar\gamma_C}{g_C n_R^{(0)}}. \tag{S5}$$

Experimentally, for real samples, all the parameters in Eqs. (S3) and (S4) are of the order of unity (for instance, in Ref. [5] the proposed values to describe certain experimental findings are following: $g_R/g_C = 2$, $\gamma_R/\gamma_C = 1.5, \varkappa = 0.9$ and the scales $\xi = 1.7$ μm and $\tau = 2.7$ ps) Further simplification can be made utilizing the quasi-stationary reservoir approximation, which according to our numerics is valid for not very small $\varkappa$. It allows to write

$$n_R(\mathbf{r}) = \frac{P(\mathbf{r})}{1 + \dfrac{\gamma_C}{\gamma_R}|A|^2}. \tag{S6}$$

The corresponding Gross-Pitaevskii-like equation reads

$$i\partial_t A = \left[-(1-i\beta)\nabla^2 + |A|^2 + \frac{g_R}{g_C}\frac{P(\mathbf{r})}{1 + \dfrac{\gamma_C}{\gamma_R}|A|^2} + \frac{i\varkappa}{2}\left(\frac{P(\mathbf{r})}{1 + \dfrac{\gamma_C}{\gamma_R}|A|^2} - 1\right)\right]A. \tag{S7}$$

Next, in our calculations, we will work in the near-threshold regime for which $|A|^2 \ll 1$. Under this condition, one can expand the denominators in Eq. (S7) as the Taylor series. Finally, we arrive at the following complex Ginzburg-Landau equation (cGLE), see Ref. [6] and references therein for review:

$$\partial_t A = \hat{\mathcal{L}}A - \left[\left(\frac{\varkappa}{2} - ig\right)\gamma P(\mathbf{r}) + i\right]|A|^2 A, \tag{S8}$$

where we explicitly separate linear and nonlinear parts,

$$\hat{\mathcal{L}} = (i+\beta)\nabla^2 + \left(\frac{\varkappa}{2} - ig\right)P(\mathbf{r}) - \frac{\varkappa}{2}, \tag{S9}$$

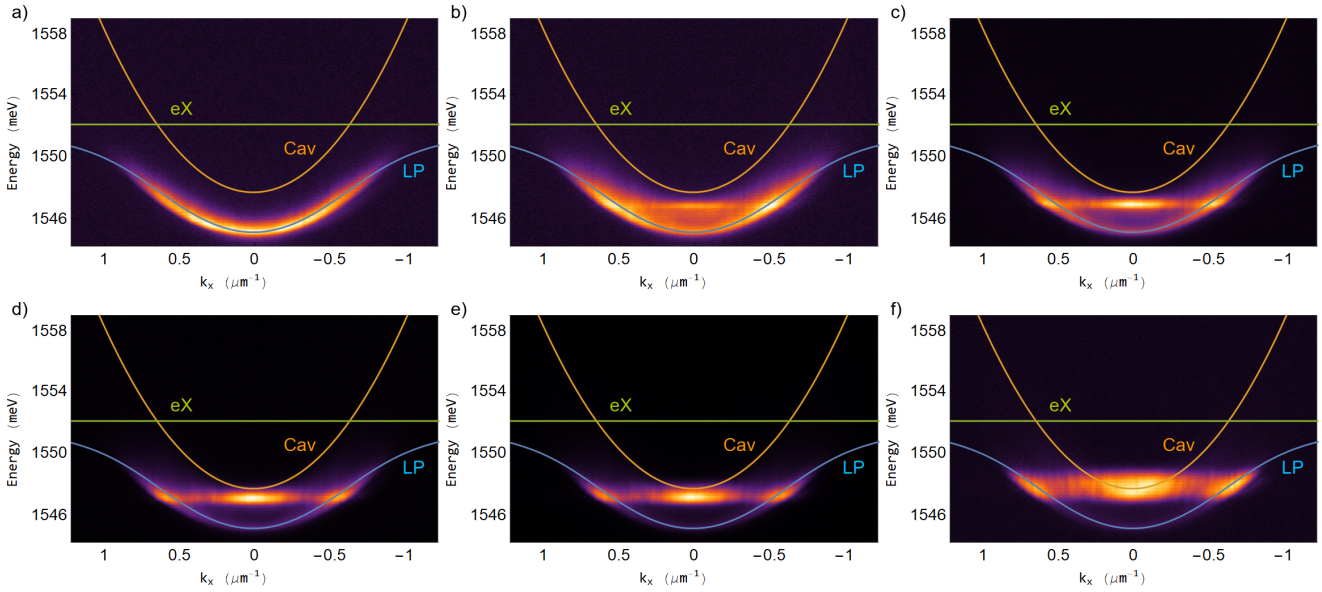

FIG. S3. Evolution of the energy-resolved emission spectrum with the pumping power growth measured for KAIST 1 sample. Here the spot size is 2.7 μm. It is smaller than the characteristic size $R_0 \approx 4.6\,\mu$m (ballistic losses regime).

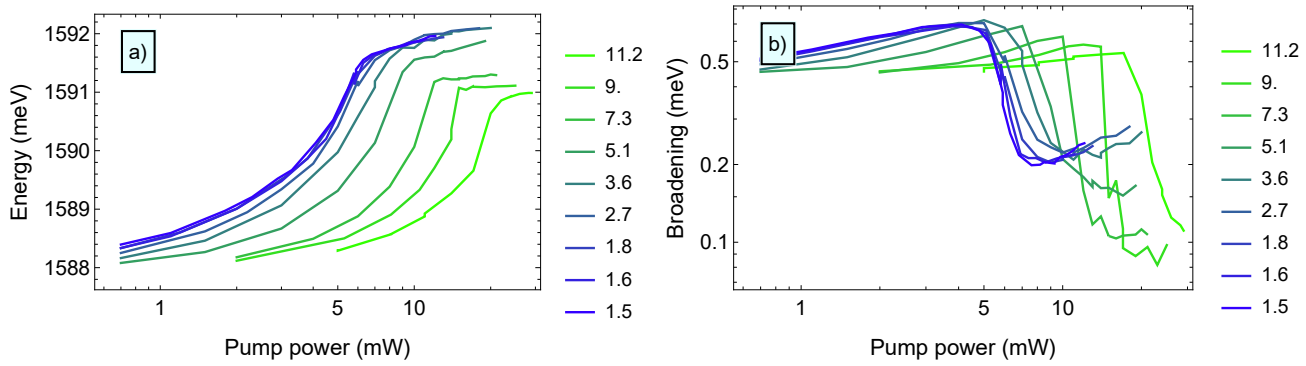

FIG. S4. KIST sample. Pump power dependencies of the emission spectrum maximum position (a) and line broadening (b) for various pump spot sizes (denoted with a bunch of colors, see the legend).

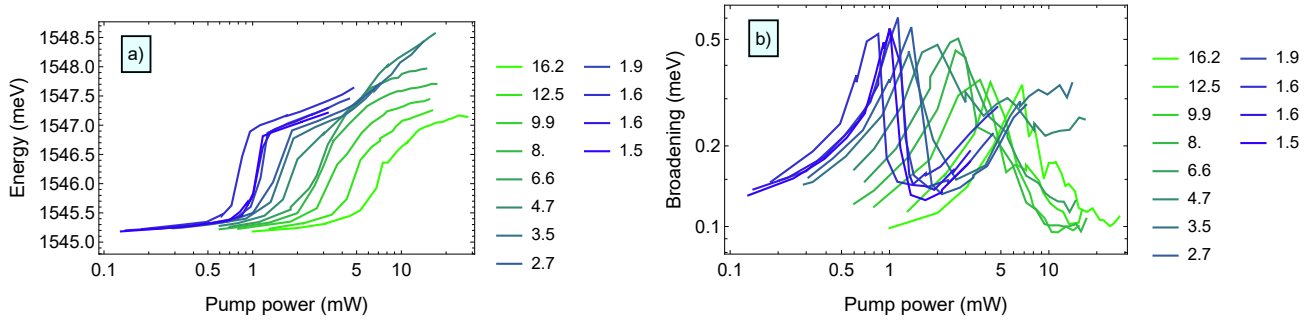

FIG. S5. KAIST 1 sample. Pump power dependencies of the emission spectrum maximum position (a) and line broadening (b) for various pump spot sizes (denoted with a bunch of colors, see the legend).

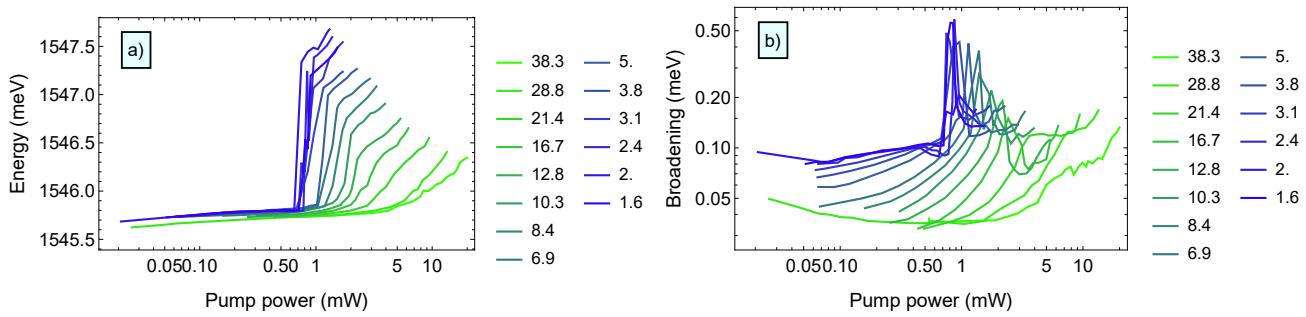

FIG. S6. KAIST 2 sample. Pump power dependencies of the emission spectrum maximum position (a) and line broadening (b) for various pump spot sizes (denoted with a bunch of colors, see the legend).

and introduce two dimensionless parameters

$$g = \frac{g_R}{g_C}, \quad \gamma = \frac{\gamma_C}{\gamma_R}. \tag{S10}$$

Here, we allow for non-uniform gain and nonlinear terms due to the space-dependent pumping profile.

The role of the β parameter is evident in the plain wave propagation away from the pumping and the condensate, where the equation (S8) can be linearized. Assuming the solution in the form $A \propto \exp\left[i(\mathbf{kr} - \omega t)\right]$, one has

$$\omega = k^2 - \frac{i}{2}(\varkappa + 2\beta k^2). \tag{S11}$$

Then, the attenuation length reads

$$l_\tau = \frac{2k}{\varkappa + 2\beta k^2}. \tag{S12}$$

It reaches maximum $l_{max} = 1/\sqrt{2\varkappa\beta}$ for $k_0 = \sqrt{\varkappa/2\beta}$. So, at $\beta \to 0$ the short-wavelength excitations propagate far away from the condensate region. Finite $\beta > 0$ suppresses this effect and makes the condensate more compact in real space (see also below).

Finally, to conclude this section, it is important to note that some authors consider models involving two consecutively filled reservoirs, inactive and active. Inactive reservoir corresponds to electron-hole plasma and high-energy excitons directly created by the laser. The active reservoir is formed by the polaritons in the so-called bottleneck of the dispersion which are scattered to the low-momentum state of the low polariton branch. The lifetime of particles in the inactive reservoir generally compares with exciton lifetimes, being hundreds of picoseconds. However, the parameters describing the active reservoir used in different papers can significantly differ. For instance, in Ref. [7] the active reservoir lifetime corresponds to that of polaritons and in Ref. [8] it rather corresponds to the exciton lifetime. Below we show how the inactive reservoir can be included in the developed above approach.

Denoting its density as n_I and the corresponding damping rate as γ_I, we can write two equations for active and inactive reservoir dynamics:

$$\partial_t n_R = W n_I - \gamma_R n_R - R_{\rm sc} n_R |\psi|^2, \tag{S13}$$

$$\partial_t n_I = P(\mathbf{r}, t) - \gamma_I n_I - W n_I. \tag{S14}$$

In the quasi-stationary approximation, one has

$$n_I = \frac{P(\mathbf{r})}{\gamma_I + W} \tag{S15}$$

and evidently, the inactive reservoir leads to a simple renormalization of the pumping in Eq. (S1)

$$P(\mathbf{r}) \to \tilde{P}(\mathbf{r}) \equiv \frac{W}{\gamma_I + W} P(\mathbf{r}), \tag{S16}$$

which only changes the related scale. Moreover, experimentally $\gamma_I \ll W$, so the factor is close to 1.

Another effect is the repulsion of condensate polaritons from the inactive reservoir particles. Assuming the same repulsion constant g_R for particles from the active and inactive reservoirs, we observe its effective renormalization

$$g_R \to \tilde{g}_R \equiv g_R \left(1 + \frac{\gamma_R}{W}\right). \tag{S17}$$

The factor in parentheses is typically $\gtrsim 1$ and can even reach values of the order of 10. However, the nonlinear term of the effective cGLE (S8) does not feel this renormalization, since its origin is the active reservoir depletion. So, we arrive at an equation similar to Eq. (S8), but where in the linear part one should use

$$\tilde{g} = \frac{\tilde{g}_R}{g_C}, \tag{S18}$$

whereas in the nonlinear term of Eq. (S8) the parameter g stays intact. Note, that the latter is substantially smaller (at least several times) than $\tilde{g}$.

Linear equation: growth rates and pumping threshold

Our study is based on the solution of Eq. (S8) for two different pumping profiles $P(\mathbf{r})$. We consider the experimentally relevant Gaussian one

$$P(r) = p_0 e^{-r^2/r_0^2}, \tag{S19}$$

numerically. Henceforth the parameter r_0 will be referred to as the spot size. In our analytics, we substitute it with the harmonic "pseudo-pumping"

$$P(r) = p_0 - p_1 r^2 \tag{S20}$$

with the same p_0 as in Eq. (S19) whereas p_1 is chosen to reproduce the curvature of the Gaussian profile,

$$p_1 = \frac{p_0}{r_0^2}. \tag{S21}$$

Qualitatively, this approximation can be justified by noting that the near-threshold condensation mainly occurs in the small vicinity of the spot center $r = 0$. So, the exact details of the pumping profile in the region where the loss term dominates are not very important, see Fig. 4 of the Main text. A comprehensive comparison between the numerics and the analytical theory will be presented below.

Now we turn to linearized equation (S8) with the pumping profile (S20). Assuming that $A \propto e^{\lambda t \pm iM\varphi}$, $M \geq 0$ (Re λ is the growth rate, $-$Im λ is the frequency, and M is the angular momentum), we have

$$\left[\lambda + \frac{\varkappa}{2} - p_0\left(\frac{\varkappa}{2} - ig\right)\right] A = (i+\beta)\left[\partial_r^2 + \frac{\partial_r}{r} - \frac{M^2}{r^2} - zr^2\right] A, \tag{S22}$$

where we use the complex parameter

$$z = p_1 \frac{\frac{\varkappa}{2} - ig}{i+\beta}. \tag{S23}$$

Next, the problem at hand can be formulated as

$$\left[\partial_r^2 + \frac{\partial_r}{r} - \frac{M^2}{r^2} - zr^2\right] A = \lambda_r A. \tag{S24}$$

which resembles a 2D harmonic oscillator in quantum mechanics. Its solution is given by

$$A = \chi(r) r^M e^{-\sqrt{z}r^2/2} \tag{S25}$$

with

$$\chi(r) = {}_1F_1\left(\frac{\lambda_r + 2(M+1)\sqrt{z}}{4\sqrt{z}}, M+1, \sqrt{z}r^2\right). \tag{S26}$$

Here ${}_1F_1$ is the Kummer's confluent hypergeometric function. Note that since we can measure the phase of z in the interval $(-\pi, 0)$, we can choose Re $\sqrt{z}$ to be positive. It is also easy to see that Re $\sqrt{z}$ grows with β making the wave function more compact in the real space. As usual, in order to have a solution with $|A|^2 \to 0$ for $r \to \infty$, one needs $\chi(r)$ to be a polynomial, hence

$$\lambda_r = -4n\sqrt{z} - 2(M+1)\sqrt{z}, \tag{S27}$$

where n is a non-negative integer. Finally,

$$\lambda(n, M) = (p_0 - 1)\frac{\varkappa}{2} - igp_0 - [4n + 2(M+1)]\sqrt{(i+\beta)\left(\frac{\varkappa}{2} - ig\right)p_1}. \tag{S28}$$

The mode with the largest growth rate, "ground state", corresponds to $n = M = 0$. We write its wave function as

$$\Psi_{0,0}(\mathbf{r}) = e^{-\sqrt{z}r^2/2}. \tag{S29}$$

In the linear theory, it can be multiplied by the arbitrary normalization constant.

Using the eigenvalues (S28) we can discuss the pumping threshold. It is defined by the condition Re $\lambda(0,0) = 0$ where we should use $p_1 = p_0/r_0^2$. It is easy to see, that we arrive at a certain quadratic equation for $\sqrt{p_0}$, which yields

$$p_{\text{TH}}(r_0) = \left(\frac{R_0}{r_0} + \sqrt{\frac{R_0^2}{r_0^2} + 1}\right)^2, \tag{S30}$$

where

$$R_0 = \frac{2\,\text{Re}\left[\sqrt{(i+\beta)\left(\frac{\varkappa}{2} - ig\right)}\right]}{\varkappa} \tag{S31}$$

is the length scale that characterizes the threshold pumping dependence on the spot size. There are two limiting cases:

$$p_{\text{TH}}(r_0) = \frac{4R_0^2}{r_0^2}, \quad r_0 \ll R_0, \tag{S32}$$

$$p_{\text{TH}}(r_0) = 1 + \frac{2R_0}{r_0}, \quad r_0 \gg R_0. \tag{S33}$$

In the physical units, the characteristic length R_0 turns into $\tilde{R}_0 = R_0\xi$, which reads

$$\tilde{R}_0 = \frac{1}{\gamma_C}\sqrt{\frac{2g_R n_R^{(0)}}{m}}\,\text{Re}\left[\sqrt{(1-i\beta)\left(1 + \frac{i\hbar\gamma_C}{2g_R n_R^{(0)}}\right)}\right] \approx \frac{1}{\gamma_C}\sqrt{\frac{2g_R n_R^{(0)}}{m}}\,\text{Re}\left[\left(1 + \frac{i\hbar\gamma_C}{2g_R n_R^{(0)}}\right)^{1/2}\right]. \tag{S34}$$

The last approximate equality is written under an assumption of $\beta \ll 1$ which is reasonable according to the existing experimental data. Importantly, $\tilde{R}_0$ depends on the polariton spectral properties namely, its curvature (mass), blueshift due to the interaction with the reservoir at the threshold, and the linewidth. So, one can see that many parameters of the considered problem *collapse* to the spectral characteristics of a single polariton state. It is also pertinent to note that the equations above allow us to predict a crossover for the condensate wave function. It is easy to see that the characteristic size of the condensate spot near the threshold follows the Gaussian one in the case of $r_0 \ll R_0$ being $\propto r_0$, whereas it scales as $\sqrt{r_0}$ if $r_0 \gg R_0$.

To conclude this section, we note that the ground state wave function (S29) violates the required asymptotic behavior at large distances from the pumping. It is not important for the threshold problem but can be crucial for other setups (e.g., a study of several pumping spots interplay). At $r \gg r_0$ the condensate is described by the following equation:

$$\left(\lambda(0,0) + \frac{\varkappa}{2}\right) A = (i+\beta)\nabla^2 A. \tag{S35}$$

Its solution describes running away from the pumping spot and decaying waves

$$A = a_0 \frac{e^{-kr}}{\sqrt{r}}, \tag{S36}$$

$$k = \sqrt{\frac{\lambda(0,0) + \frac{\varkappa}{2}}{i+\beta}}. \tag{S37}$$

Here k is the asymptotic wave number. Constant A_0 should be chosen so that the functions (S29) and (S36) match each other at some point $r \sim r_0$. For instance, taking $r = r_0$, one has

$$a_0 = \sqrt{r_0} e^{kr_0 - \sqrt{z} r_0^2/2}. \tag{S38}$$

Justification of the pseudo-pumping approximation

To test the pseudo-pumping theory, we compare its predictions with the ones of a numerical solution of the linear problem with the Gaussian pumping profile. We find that the approximation works well if the repulsion parameter g is not very large. Particular comparison results are shown in Fig. S7. We observe an excellent agreement with the relative error defined as

$$\delta p_{\text{TH}}(r_0) = \frac{p_{\text{GAUSS}}(r_0) - p_{\text{TH}}(r_0)}{p_{\text{TH}}(r_0)} \tag{S39}$$

being $\lesssim 0.01$ (here $p_{\text{GAUSS}}(r_0)$ is the numerically obtained threshold for the Gaussian pumping profile).

In the opposite case of $g \gg 1$, the qualitative picture is as follows: polaritons feel a strong repulsion from the pumping spot region where the density of reservoir particles is high, and they tend to escape that region. Hence, the condensate wave function essentially spreads in the direct space leaving the domain, where the Gaussian and harmonic profiles match each other well. Consequently, our theory loses its accuracy and predictive power.

In other words, large $g \gg \varkappa$ can cause troubles since a strong repulsion from the reservoir can prevent the "ground state" condensation. To have some intuition on this phenomenon, let us present some arguments. If $g \gg \varkappa$, $\beta \ll 1$, then

$$z \approx -p_1 g(1+i\beta),\ \sqrt{z} \approx -i\sqrt{g p_1} + \sqrt{g p_1}\beta/2. \tag{S40}$$

Evidently, in this case, $\sqrt{z}$ is mostly imaginary (for $\beta = 0$ its real part is zero), so the wave function spatial decay is slow. To have a good correspondence with the Gaussian spot results, we better have $\sqrt{z} \gtrsim 1/r_0^2$, which gives us an inequality (bearing in mind that $p_1 = p_0/r_0^2$)

$$\sqrt{g p_0}\beta r_0 \gtrsim 1, \tag{S41}$$

which shows us that β cannot be too small. We can proceed near the threshold with the usage of pumping $p_{\text{TH}}(r_0)$. Under the same assumptions ($g \gg \varkappa$, $\beta \ll 1$) one has $R_0 \approx 2\sqrt{g}/\varkappa$ and we arrive at the conditions

$$\begin{aligned} \frac{\beta g}{\varkappa} &\gtrsim 1, \quad r_0 \ll R_0, \\ \beta r_0 \sqrt{g} &\gtrsim 1, \quad r_0 \gg R_0. \end{aligned} \tag{S42}$$

Hence, even for large g, the diffusion parameter β can lead to condensation to the compact Gaussian ground state (S29) if it is not very small. Numerically, we observe that these criteria work semi-quantitatively, see Fig. S8 for a particular example.

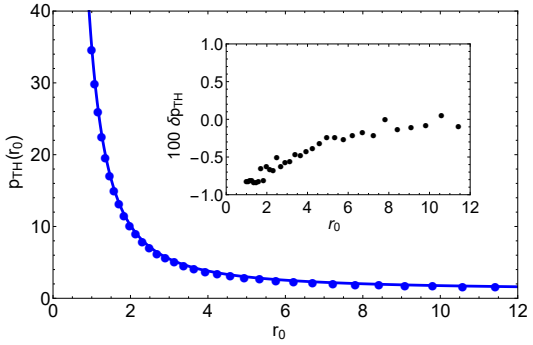

FIG. S7. Threshold pumping power for the Gaussian pumping (blue dots obtained numerically) and for the parabolic one [blue line, see Eq. (S30)] for various spot sizes r_0. The characteristic length scale $R_0 \approx 2.9$. Inset shows the relative error of the analytical prediction multiplied by the factor 100. The parameters are $g = 2$, $\gamma = 1$, $\varkappa = 1$, and $\beta = 0.1$.

Sets of parameters

Before turning to the nonlinear problem, it is pertinent to discuss possible sets of parameters relevant to semiconducting multiple quantum well microresonators. Importantly there is a vast space of considered by different groups parameters for the studied samples. Below we will focus on those of Refs. [5, 9].

In the first paper [5], the authors successfully described the experimental observations in the structure based on AlGaAs using the following set:

$$\begin{aligned} &m = 5 \times 10^{-5} m_e,\ E_{\text{Pol}} = 1.6\,\text{meV}, \\ &g_C = 6 \times 10^{-3}\,\text{meV}\,\mu\text{m}^2,\ g_R = 2g_C, \\ &\gamma_C = 0.33\,\text{ps}^{-1},\ \gamma_R = 1.5\gamma_C. \end{aligned} \tag{S43}$$

For spot with $r_0 = 10\,\mu\text{m}^2$ the reported pumping threshold is $P_{\text{TH}} = 25$ mW with conversion efficiency $\approx 24\%$. Next, we assume that this pumping threshold is x times larger than the one for homogeneous pumping (x is directly related to the R_0 parameter of our theory). So, $n_R^{(0)} = p_{\text{TH}}(r_0)/\gamma_R x$ and we can write the equation for x:

$$x = \frac{1}{\gamma_C}\sqrt{\frac{2g_R n_R^{(0)}}{m}}\,\text{Re}\left[\left(1 + \frac{i\hbar\gamma_C}{2g_R n_R^{(0)}}\right)^{1/2}\right]. \tag{S44}$$

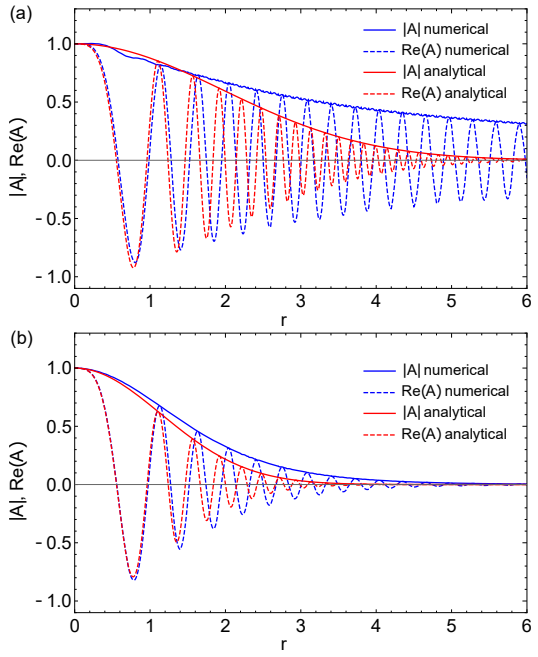

FIG. S8. Here we compare solutions of the linear equations for strong repulsion $g = 10$ and small pumping spot size $r_0 = 2$. (a) $\beta = 0.001$. The results for the Gaussian pumping and the parabolic one are essentially different. Moreover, in the Gaussian case, there are many other modes with close growth rates including those with nonzero angular momentum M. The pumping threshold prediction (S30) fails in this case. (b) $\beta = 0.1$ "stabilizes" the condensate making the "pseudo-pumping" approximation applicable. Other parameters in both panels are $\gamma = 1$, $\varkappa = 1$

The solution is $x \approx 2.8$. Using this value we get

$$\varkappa = 0.9,\ g = 2,\ \gamma = 2/3. \tag{S45}$$

We also can calculate the blueshift at the threshold for the homogeneous pumping $g_R n_R^{(0)} \approx 0.5$ meV and $R_{\rm SC} \approx 0.01\,\mu{\rm m}^2/{\rm ps}$ both being reasonable values.

In the second paper [9], the authors present all the required parameters including those describing the inactive reservoir (which evidently leads to more ambiguity in their values). After simple calculations one gets

$$\varkappa = 53.7,\ g = 26.5,\ \gamma = 1, \tag{S46}$$

and homogeneous pumping blueshift ≈ 0.06 meV. The last value seems to be anomalously small whereas g and $\varkappa$ are anomalously big. Theoretically, for these "extreme" parameters, our approach is inapplicable (the Stuart-Landau equation leads to unbounded growth of the condensate amplitude, see below) and numerical analysis shows the condensate collapse to a very narrow spot. We do not consider such "anomalous" parameters in detail here. However, we would like to note that it will be interesting to measure the pumping threshold curve for the corresponding sample which can possibly lead to refining of the parameters. Another possibility here can be that these "anomalous" values are indeed required to observe very long-range synchronization of two condensate spots for distances $\sim 100\,\mu$m. The corresponding analysis is out of the scope of the present study.

Weakly nonlinear analysis

According to the linear theory for pseudo-pumping and comparison with numerics for the Gaussian pumping spot, we see that the condensation typically occurs to the ground state (S29). Near the threshold, all other states have negative growth rates and their contribution to the condensate wave function is negligible.

To be precise, let us write the solution of the nonlinear problem as

$$A(\mathbf{r},t) = [A_0(t)\Psi_{0,0}(\mathbf{r}) + w(\mathbf{r},t)]\, e^{-i\lambda'' t}. \tag{S47}$$

Here and below, we use the notation

$$\lambda(0,0) = \lambda' - i\lambda'', \tag{S48}$$

and assume that $\lambda' \ll 1$. After plugging (S47) to Eq. (S8) the explicit phase factor of the former is equivalent to a substitution $\hat{\mathcal{L}} \to \hat{\mathcal{L}}' = \hat{\mathcal{L}} + i\lambda''$. Standard arguments allow predicting the following "hierarchy": $A_0 \sim \sqrt{\lambda'}$, $\partial_t A_0 \sim (\lambda')^{3/2}$, hence $w \sim A^3 \sim (\lambda')^{3/2}$ and $\partial_t w \sim (\lambda')^{5/2}$. The latter can be neglected with the accuracy of our calculations. So, we obtain

$$\begin{aligned}\hat{\mathcal{L}}' w = {} & \Psi_{0,0}\partial_t A_0 - \lambda'\Psi_{0,0}A_0 \\ & - \left[\left(\frac{\varkappa}{2} - ig\right)\gamma P(r) + i\right] |A_0|^2 A_0 |\Psi_{0,0}|^2 \Psi_{0,0}.\end{aligned} \tag{S49}$$

Then, we multiply both sides of this equation by $\Psi_{0,0}$ (which is the complex conjugate of the adjoin operator eigenfunction, $\hat{\mathcal{L}}'^*$ in our case since $\hat{\mathcal{L}} = \hat{\mathcal{L}}^T$) and note that

$$\int \Psi_{0,0}\hat{\mathcal{L}}' w d^2\mathbf{r} = \int w\hat{\mathcal{L}}'\Psi_{0,0} d^2\mathbf{r} \sim (\lambda')^{5/2} \tag{S50}$$

is negligible (this is the solvability condition for our problem). Finally, we arrive at the Stuart-Landau equation

$$\partial_t A_0 = \lambda' A_0 - c|A_0|^2 A_0, \tag{S51}$$

where

$$c = ic_1 + c_2\left(\frac{\varkappa}{2} - ig\right)\gamma \equiv c' + ic'', \tag{S52}$$

$$c_1 = \frac{\int_0^\infty r|\Psi_{0,0}(r)|^2\Psi_{0,0}^2(r)dr}{\int_0^\infty r\Psi_{0,0}^2(r)dr}, \tag{S53}$$

$$c_2 = \frac{\int_0^\infty rP(r)|\Psi_{0,0}(r)|^2\Psi_{0,0}^2(r)dr}{\int_0^\infty r\Psi_{0,0}^2(r)dr}. \tag{S54}$$

Here we explicitly used azimuthal symmetry of the pumping profile. Importantly, thus defined $c_{1,2}$ are not necessarily positive reals but usually are certain complex numbers.

The solution of Eq. (S51) for $c' > 0$ is well-known. For the amplitude one has

$$|A_0(t)|^2 = \left[\frac{c'}{\lambda'}\left(1 - e^{-2\lambda' t}\right) + |A_0(t=0)|^{-2}e^{-2\lambda' t}\right]^{-1}. \tag{S55}$$

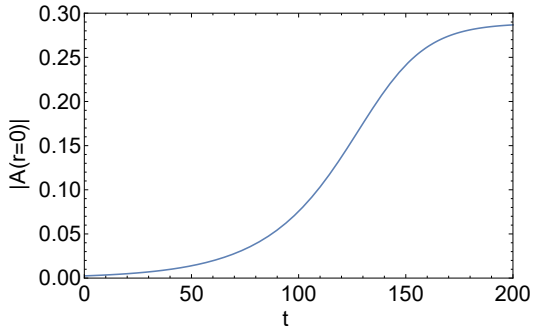

FIG. S9. Time evolution of the condensate wave function amplitude at the center of the pumping profile obtained from the Stuart-Landau equation (S51) for a particular parameter set.

Asymptotically, at $t \gg 1/\lambda'$

$$|A_0(t \to \infty)| = \sqrt{\lambda'/c'}, \tag{S56}$$

whereas the phase growth linearly with the frequency $c''\lambda'/c'$. Also using the definition (S47), we have a condensate frequency

$$\omega_0 = \lambda'' + c''\lambda'/c'. \tag{S57}$$

Near the threshold, the last term here provides a small correction $\propto p_0 - p_{\rm TH}$. In the particular case of a large pumping spot $r_0 \gg R_0$, one has $p_1 \ll 1$ and the frequency (strictly speaking, its blueshift) of the polariton line is just g, which corresponds to the expected result $\omega_0 = g_R n_R^{(0)}/\hbar$ in physical units [cf. Eq. (S28)].

For the parabolic pseudo-pumping, we know the exact form of the wave function (S29) and thus can calculate the coefficients c', c''. After some calculations, we have

$$c_1 = \frac{\sqrt{z}}{\sqrt{z} + \mathrm{Re}\sqrt{z}}, \tag{S58}$$

$$c_2 = \frac{\sqrt{z}\,[p_0(\sqrt{z} + \mathrm{Re}\sqrt{z}) - p_1]}{(\sqrt{z} + \mathrm{Re}\sqrt{z})^2}. \tag{S59}$$

These equations allow for analytical prediction of the c dependence on the system parameters. In particular, the boundary between $c' > 0$ and $c' < 0$ can be determined.

We illustrate the results of the analytical theory in Fig. S9. The used parameters are $g = 2$, $\varkappa = 1$, $\gamma = 1$, $\beta = 0.1$, $p_0 = 1.85$, $r_0 = 10$. Condensate amplitude at $r = 0$ saturates at value $|A_0| \approx 0.29$. The semi-analytical approach with numerically obtained ground state wave function for the Gaussian pumping yields $|A_0| \approx 0.32$. The numerical solution of cGLE (S8) on a lattice results in $|A_0| \approx 0.33$; without the Taylor expansion [see Eq. (S7)] the corresponding quantity is $|A_0| \approx 0.32$. Finally, simulating two coupled equation (S3) and (S4) we get $|A_0| \approx 0.35$. In all the cases, the time of the condensate formation $\sim 100\tau \sim 100$ ps in physical units.

In the case $c' < 0$, the condensate wave function determined by Eqs. (S47) and (S51) "blows up" and our theory

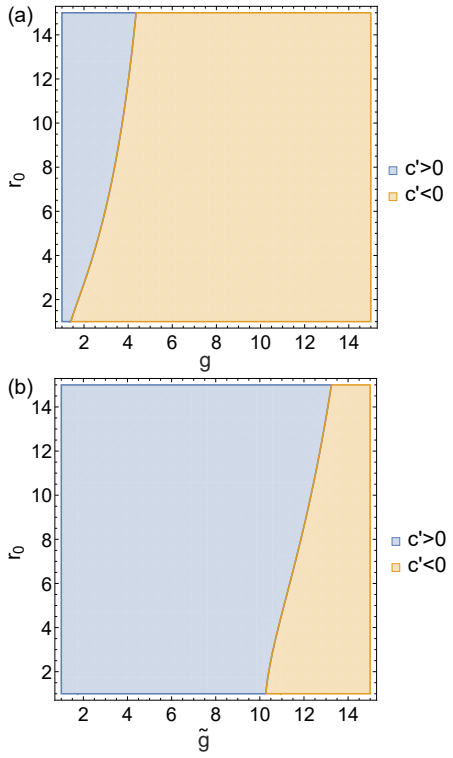

FIG. S10. When considering the properties of the nonlinear equation on the plane "repulsion from the reservoir – pumping spot size" in the near-threshold regime, the crucial property is the sign of c' parameter. For large enough g the region with $c' < 0$ where the Stuart-Landau equation (S51) is inapplicable is quite large, see panel (a). However, if we connect strong repulsion with the inactive reservoir particles thus using renormalized $\tilde{g}$, we will get a smaller constant g in the nonlinear term. In panel (b) $\tilde{g} = 2g$, and the boundary of the $c' < 0$ region is pushed towards much stronger repulsions. The parameters used in both panels are $\gamma = 1$, $\varkappa = 1$, and $\beta = 0.1$.

based on the condition $|A|^2 \ll 1$ is inapplicable. This case deserves a separate study. Here we just want to point out that it was not observed in our experiments. A possible source of negative c' values can be a strong repulsion between the condensate and the reservoir. In this case, they tend to spatially separate, which can lead to the formation of a narrow profile of the dense condensate at the center of the pumping spot and significant reservoir depletion. So, a certain "autolocalization" of the condensate occurs and its wave function is subject to a "collapse" [10]. It is pertinent to note that the theory of the pumping threshold is still applicable in this case.

In the developed formalism, we can discuss the boundary separating $c' > 0$ and $c' < 0$ regimes using explicit equations (S58) and (S59) determining the c parameter. As previously, to have some intuition we shall use a large g expansion and the threshold value of p_0 for pumping spots of various sizes r_0. After some calculations, in the case of $r_0 \ll R_0$, we have

$$c' \approx \frac{\gamma\varkappa}{2} - \frac{4\gamma g}{\varkappa r_0^2}. \tag{S60}$$

For large pumping spots with $r_0 \gg R_0$, we obtain

$$c' \approx \frac{\gamma\varkappa}{2} - \frac{\gamma\beta g}{2} \tag{S61}$$

under the assumption $\sqrt{g}/r_0 \gg 1$ and trivial result

$$c' \approx \frac{\gamma\varkappa}{2} \tag{S62}$$

in the opposite case. In both limiting cases of small and large spots, we see that large enough g will lead to negative c' and, hence, a regime where the Stuart-Landau equation (S51) is inapplicable.

At this point, it is pertinent to discuss the possible origins of large $g = g_R/g_C$ values. In the case of the single reservoir approach, its value is limited by the polariton Hopfield coefficients [11]. However, if we take the inactive reservoir into consideration, the situation drastically changes (see the discussion above). The g parameter in the nonlinear term of Eq. (S8) is substantially smaller than that of the linear theory. This leads to shrinkage of the parameter region where c' is negative. For a particular parameter set it is illustrated in Fig. S10, where the result without inactive reservoir and with it ($\tilde{g} = 2g$) are contrasted on the $g - r_0$ plane. We conclude, that accounting for the inactive reservoir leads to the prevailing of the $c' > 0$ region where the Stuart-Landau equation can be used for the condensate dynamics description. Nevertheless, we note that even if this "stabilization" of the smooth Gaussian condensate takes place, at higher pumpings p_0 above the threshold it can become unstable (especially near the boundary $c' = 0$) leading to the condensate "collapse". A detailed study of this issue is out of the scope of the present paper.

[1] J. Kasprzak, M. Richard, S. Kundermann, A. Baas, P. Jeambrun, J. M. J. Keeling, F. Marchetti, M. Szymańska, R. André, J. Staehli, *et al.*, Bose–einstein condensation of exciton polaritons, Nature **443**, 409 (2006).

[2] M. Wouters and I. Carusotto, Excitations in a nonequilibrium bose-einstein condensate of exciton polaritons, Phys. Rev. Lett. **99**, 140402 (2007).

[3] I. Carusotto and C. Ciuti, Quantum fluids of light, Reviews of Modern Physics **85**, 299 (2013).

[4] D. Solnyshkov, H. Tercas, K. Dini, and G. Malpuech, Hybrid Boltzmann–Gross-Pitaevskii theory of Bose-Einstein condensation and superfluidity in open driven-dissipative systems, Physical Review A **89**, 033626 (2014).

[5] G. Roumpos, M. D. Fraser, A. Löffler, S. Höfling, A. Forchel, and Y. Yamamoto, Single vortex–antivortex pair in an exciton-polariton condensate, Nature Physics **7**, 129 (2011).

[6] I. S. Aranson and L. Kramer, The world of the complex ginzburg-landau equation, Reviews of modern physics **74**, 99 (2002).

[7] I. Gnusov, S. Harrison, S. Alyatkin, K. Sitnik, H. Sigurdsson, and P. G. Lagoudakis, Vortex clusters in a stirred polariton condensate, arXiv preprint arXiv:2308.09373 (2023).

[8] D. Choi, M. Park, B. Y. Oh, M.-S. Kwon, S. I. Park, S. Kang, J. D. Song, D. Ko, M. Sun, I. G. Savenko, *et al.*, Observation of a single quantized vortex vanishment in exciton-polariton superfluids, Physical Review B **105**, L060502 (2022).

[9] J. D. Töpfer, H. Sigurdsson, L. Pickup, and P. G. Lagoudakis, Time-delay polaritonics, Communications Physics **3**, 2 (2020).

[10] L. Dominici, M. Petrov, M. Matuszewski, D. Ballarini, M. De Giorgi, D. Colas, E. Cancellieri, B. Silva Fernández, A. Bramati, G. Gigli, *et al.*, Real-space collapse of a polariton condensate, Nature Communications **6**, 8993 (2015).

[11] J. J. Hopfield, Theory of the contribution of excitons to the complex dielectric constant of crystals, Phys. Rev. **112**, 1555 (1958).